A PROCESSING PIPELINE FOR CRISM HYPERSPECTRAL MAPPING DATA. M. S. Phillips[1], S. L. Murchie[1], F. P. Seelos[1], K. M. Hancock[1], D. C. Stephens[1], M. Kawamura[1,2]. [1]Johns Hopkins University Applied Physics Laboratory (Michael.Phillips@jhuapl.edu), [2]Department of Physics and Astronomy, Dartmouth.

Introduction: Results from both the Compact Reconnaissance Imaging Spectrometer for Mars (CRISM) and the Observatoire pour la Minéralogie, l'Eau, les Glaces et l'Activité (OMEGA) instruments have shown that the type and abundance of alteration minerals on Mars varies with surface age [1]–[7]. Although the general story of secular variation in alteration mineralogy has come into focus, detailed questions remain about the spatial variation and extent of alteration on Mars that cannot be answered with low spectral resolution products with near global coverage (e.g., CRISM MRDR multispectral map tiles) or high spectral resolution products with low spatial coverage (e.g., CRISM targeted observations). To fill the gap between global multispectral and targeted hyperspectral products, we have developed a processing pipeline for CRISM 180-m/pixel, 262-channel hyperspectral mapping data (HSP) – a dataset that affords better spatial coverage compared to targeted observations (~39% vs. ~2% global coverage) and increased spectral sampling over multispectral mapping data (MSP).

Background. A data processing pipeline was recently completed for MRDR map tiles that are currently being delivered to the PDS [8]. The development of this pipeline updated our knowledge on 5 steps required to process HSP data to a state at which standard CRISM spectral parameters [9] can be applied and the data can be interpreted: (1) radiometric calibration correction, (2) remediation of noise using a filtering algorithm, (3) normalization of atmospheric gas absorptions, (4) photometric correction for solar incidence angle, and (5) reconciliation of inter-strip differences in calibration and atmospheric opacity. Steps (1), (2), and (5) have been developed in this effort for HSP-specific processing while steps (3) and (4) are standard capabilities of the publicly available CRISM Analysis Toolkit [10].

Methods: *Radiometric Calibration Correction.* CRISM targeted observations (FRT, HRL, HRS, FRS, ATO, ATU) and VNIR-IR mapping data (MSP and HSP) are acquired at different frame rates, and there are small differences in radiometric calibration with frame rate. CRISM's radiometric calibration is based on fully hyperspectral data that were acquired at the frame rate of targeted observations, and that wavelength-dependent calibration vector is subset to the wavelengths used in any particular observing mode. Hence, a correction for the higher frame rate of HSP data must be derived to make the hyperspectral information in the HSP data comparable to the information in targeted observations. To develop the correction for frame-rate-dependence of radiometric calibration, we used a nadir-pointed observation of Tharsis that was collected for flat-field correction of targeted observations, averaging many frames along-track, and ratioed it to an overlapping, similarly processed HSP data strip.

Noise Remediation Filtering. A new noise remediation approach for HSP data is a second major development in this effort. CRISM data contain two types of noise: (i) systematic noise that depends on cross-track optical artifacts and calibration residuals at specific detector elements, and (ii) for the IR detector, stochastic noise due to operation at temperatures 5-15K warmer than the design temperature. Corrections for systematic noise in HSP data are adapted directly from the CRISM processing pipeline.

For remediation of stochastic noise, we developed a variation of the filtering approach applied to MSP data [8]. The MSP filtering algorithm rasters a 2D kernel over each band of the conditioned image cube, calculating outlier values within the kernel and counting each instance a pixel is flagged as an outlier. Pixels counted as outliers above a threshold value are updated through a distance-weighted spatial interpolation. This process is iterated until all outlier pixels have been updated. The MSP "iterative outlier voting" routine is applied individually to each wavelength because small band-to-band variations may contain signal. However, the continuous spectral sampling of HSP data makes valid the assumption of band-to-band correlation. We therefore extended the filtering kernel to 3 dimensions and applied the same "iterative outlier voting" technique to HSP data (Fig. 1A,B).

Stochastic noise in IR data is wavelength dependent with longer wavelength bands impacted more severely by high detector temperatures than shorter wavelength bands. In the most egregious cases, spatial structure is indiscernible making a statistical approach to noise remediation untenable (Fig. 1A). We therefore adopted a hybrid filtering approach in which the iterative outlier voting filter, is applied to wavelengths 1021.00 to 2641.74 nm (approximately filtering zones 1 and 2 of the CRISM IR detector [1]) and the "non-local meets global" (denoiseNGMeet) denoising and restoration algorithm [11] is applied to wavelengths > 2641.74 nm (approximately filtering zone 3 of the CRISM IR detector [1]). The denoiseNGMeet algorithm leverages both spatial and spectral correlations of a hyperspectral image to remediate noise and restore spatial structure with non-local low-rank tensor approximation [11].

Inter-Strip Radiometric Reconciliation. Variations in atmospheric and instrument state result in radiometric discrepancies between individual CRISM mapping strips. The relatively high density of spatial overlap between MRDR data in enables a wavelength-dependent correction to reconcile component strips into a consistent radiometric framework tied to the highest quality data [8]. HSP data are sparsely connected spatially compared to the MRDR dataset, making this approach to achieving a consistent radiometric framework for the HSP data alone infeasible. Instead, we leverage the inclusion of HSP data (albeit reduced to the MSP wavetable) in the MRDR tile dataset. Our approach was to fit a surface across all wavelengths shared between the hyperspectral HSP and MRDR HSP data using a Multi-Layer Perceptron (MLP) regressor [12]. With this surface fit we apply a matrix transformation to the HSP data into the radiometrically reconciled space of the MRDR HSP data.

Results: We have tested our processing pipeline on CRISM map tile T0932 over Candor Mensa (4°50'S, 75°50' W). Figure 1 shows results from processing using two endmember filtering options: (i) an iterative outlier voting filter applied only in the spatial dimension (the approach used on MRDR data, Fig. 1C 'FLT0'); (ii) the denoiseNGMeet algorithm applied to all wavelengths of the HSP data (Fig. 1C 'NGM'). We are processing the hybrid filtering approach delineated in our methods (Fig. 1A,B) at the time of writing and these results will be presented at the conference.

Discussion: Newly processed HSP mapping data will enable fresh insights into questions that cannot be answered with CRISM MRDR or targeted data alone. For example: how widespread are deeply buried occurrences of pre-Noachian Ca/Fe carbonate, and what does their occurrence imply for the chemistry of early wet environments? How continuous is alteration at depth, and what is the balance of alteration to hydrated silica vs. phyllosilicate? What is the distribution of phases that imply high alteration temperatures (epidote, prehnite), and what does the answer imply for early Martian evolution? We will investigate these questions in upcoming work featuring the HSP mapping dataset.

References: [1] S. Murchie et al., *JGRP*, *112*(E5), 2007. [2] S. L. Murchie et al., *JGRP*, *114*(E2), 2009. [3] J. F. Mustard et al., *Nature*, *454*(7202), pp. 305–309, 2008. [4] J. Carter, et al., *JGRP*, *118*(4), 831–858, 2013. [5] J.-P. Bibring et al., *Science*, *312*(5772), 400, 2006. [6] J.-P. Bibring et al., *Mars Express: The Scientific Payload*, 2004, *1240*, 37–49. [7] B. L. Ehlmann et al., *Nat. Geo.*, *1*(6), 355, 2008. [8] F. P. Seelos, et al., LPSC 2019 Abstract #2635. [9] C. E. Viviano-Beck et al., *JGRP*, *119*(6), 1403–1431, 2014. [10] S. L. Murchie et al., *JGRP*, *114*, 2009. [11] W. He et al., *IEEE Trans. Pattern Anal. Mach. Intell.*, *44*(4), 2089–2107, 2022. [12] M. S. Phillips, et al., LPSC 2022, Abstract#1487.

Acknowledgements: This work was supported by NASA MDAP Grant #80NSSC17K0534

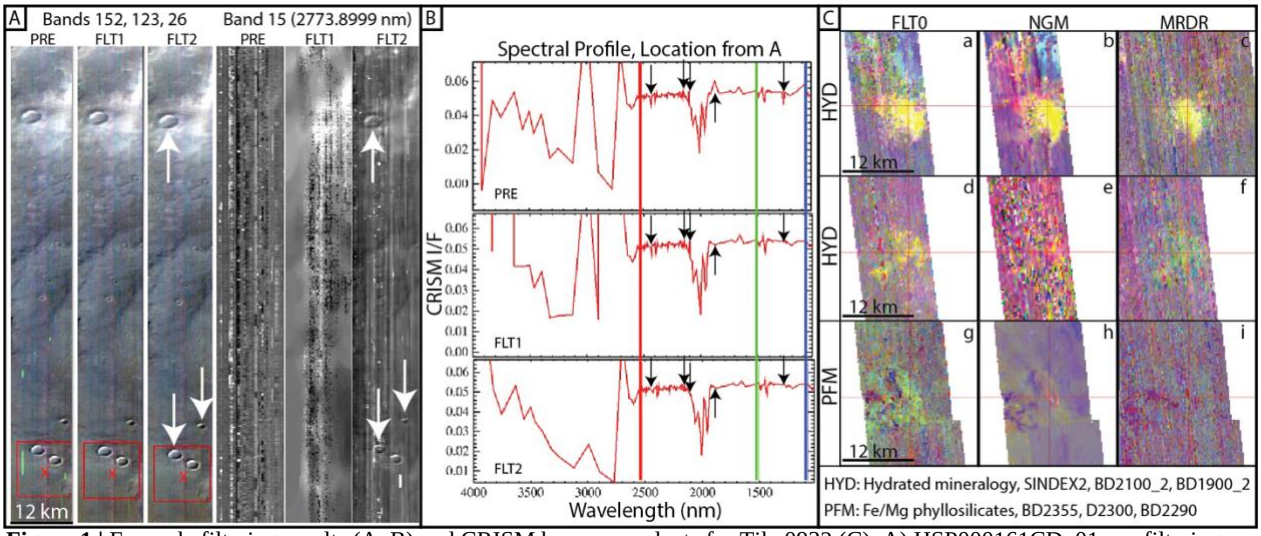

Figure 1 | Example filtering results (A, B) and CRISM browse products for Tile 0932 (C). A) HSP000161CD_01 pre-filtering (PRE), and filtered with a 3D iterative outlier voting filter (IOVF) on the entire image cube (FLT1) and with the denoiseNGMeet routine at wavelengths >2641.74 nm (FLT2). Band 15 shows the advantage of the denoiseNGMeet routine for spatial restoration of egregiously noisy bands. White arrows indicate examples of spatial restoration through the denoiseNGMeet routine. B) Spectral profiles from the red 'x' in A. Black arrows indicate examples where noise has been remediated. Note the improved quality of the >2641.74-nm region for FLT2. C) Example HSP (a, b, d, e, g, h) and MRDR (c, f, i) browse products generated after processing through the full HSP pipeline. Each row shows the same location. FLT0: filtered using the 2D IOVF; NGM: filtered with denoiseNGMeet routine; MRDR: multispectral map tile. HSP browse products reveal more detailed compositional variations than MRDR products. Final results using FLT2 will be presented at the conference.